



ELSEVIER

Available online at [www.sciencedirect.com](http://www.sciencedirect.com)  
SCIENCE @ DIRECT®

Nuclear Instruments and Methods in Physics Research A 497 (2003) 129–134

NUCLEAR  
INSTRUMENTS  
& METHODS  
IN PHYSICS  
RESEARCH  
Section A

[www.elsevier.com/locate/nima](http://www.elsevier.com/locate/nima)

## A dedicated system for breast cancer study with combined SPECT–CT modalities

A. Del Guerra<sup>a,\*</sup>, G. Di Domenico<sup>b</sup>, A. Fantini<sup>b</sup>, M. Gambaccini<sup>b</sup>, L. Milano<sup>b</sup>, N. Sabba<sup>b</sup>, A. Taibi<sup>b</sup>, A. Tartari<sup>b</sup>, A. Tuffanelli<sup>b</sup>, G. Zavattini<sup>b</sup>, R. Pani<sup>c</sup>, R. Pellegrini<sup>c</sup>, A. Soluri<sup>c</sup>, M.N. Cinti<sup>c</sup>, A. Bevilacqua<sup>d</sup>, D. Bollini<sup>d</sup>, M. Gombia<sup>d</sup>, N. Lanconelli<sup>d</sup>, F. Arfelli<sup>e</sup>, R. Longo<sup>e</sup>, A. Olivo<sup>e</sup>, S. Pani<sup>e</sup>, P. Poropat<sup>e</sup>, L. Rigon<sup>e</sup>

<sup>a</sup> Department of Physics, University of Pisa and INFN Sezione di Pisa, Via F. Buonarroti 2, 56127 Pisa, Italy

<sup>b</sup> Department of Physics, University of Ferrara and INFN Sezione di Ferrara, via Paradiso 12, 44100 Ferrara, Italy

<sup>c</sup> Department of Experimental Medicine, University of Rome La Sapienza, viale Regina Elena 324, 00161 Rome, Italy

<sup>d</sup> Department of Physics, University of Bologna and INFN Sezione di Bologna, via C. Berti Pichat 6/2, 40127 Bologna, Italy

<sup>e</sup> Department of Physics, University of Trieste and INFN Sezione di Trieste, via Valerio 2, 34127 Trieste, Italy

### Abstract

A prototype of a combined CT–SPECT tomograph for breast cancer study has been developed and evaluated. It allows to perform scintimammography and X-ray CT in the same geometrical conditions. The CT system is based on a quasi-monochromatic beam tuned at 28 keV and an array of ultra fast ceramic scintillators coupled to photodiodes whilst the SPECT system is based on two scintillator matrices coupled to position sensitive photomultipliers. CT and SPECT sinograms of a test phantom were recorded and reconstructed with both modalities. Image fusion of CT and SPECT images was then performed. The developed CT–SPECT prototype is able to detect a region of interest of 1 cm<sup>3</sup>, with a 10:1 tumour/background concentration ratio, within an object having a diameter of 8 cm.

© 2002 Elsevier Science B.V. All rights reserved.

PACS: 87.59.–e; 87.59.Fm; 87.59.Ta; 87.62.+n

Keywords: Breast cancer; Computed tomography; Scintimammography; Image fusion

### 1. Introduction

Although conventional mammography is the most widespread technique in clinical practice, its limitations in terms of specificity and sensitivity are well known [1,2]. To improve the diagnostic

information scintigraphic techniques have been used, and in particular scintimammography with an Anger camera [3,4]. The recent introduction of dedicated imagers with small field of view (FOV) coupled to a moderate breast compression has allowed to increase the sensitivity up to 80% for tumour size between 0.5 and 1 cm [5]. An alternative technique has also been proposed with the breast in a pendular prone position and a dedicated ring for its SPECT imaging. It has been

\*Corresponding author. Tel.: +39-050-2214942; fax: +39-050-2214333.

E-mail address: [delguerra@pi.infn.it](mailto:delguerra@pi.infn.it) (A. Del Guerra).

suggested that a dedicated CT system could be of great benefit if combined with this SPECT modality. Indeed, by integrating the morphological image with the functional one, the sensitivity for lesions smaller than 1 cm could be further increased.

An integrated CT–SPECT system for breast cancer study is being investigated as a large research program of Italian universities [6,7]. A dedicated tomographic imager has been assembled at the Physics Department of Ferrara University which allows us to perform scintimammography and X-ray CT in the same geometrical conditions. Preliminary system performance will be here reported together with present limitations and future improvements.

## 2. Materials and methods

The experimental set-up is schematically shown in Fig. 1. The system, whose toroidal ring has a diameter of about 13 cm, has been designed and built in order to image patients in a pendular

prone position (leaning breast). In the prototype, two SPECT detectors are orthogonally positioned to the X-ray source-to-CT detector axis and have been mounted on the same rotating gantry. The X-ray source produces a quasi-monochromatic beam tuned at 28.5 keV ( $\Delta E/E \approx 4\%$ ), with a measured flux of  $1.7 \times 10^4 \text{ photons mm}^{-2} \text{ s}^{-1} \text{ mA}^{-1}$ . A radiograph of the beam taken on the object plane is shown in Fig. 2. Details of the monochromator system have been presented elsewhere [6].

### 2.1. CT detector

The X-ray detector is based on an array of Ultra Fast Ceramic (UFC) scintillators coupled to photodiodes (manufactured by Siemens, Germany) [8]. Each UFC module consists of 16 elements,  $1 \times 20 \text{ mm}^2$  of size. Nine modules were employed to assemble the detector to form an array of 144 elements. An ad hoc electronics was developed at the University of Ferrara to read out the photocurrent of each channel. Nine circuit boards, based on dual current input ADCs (Burr-Brown, USA, mod.DDC112), performed current

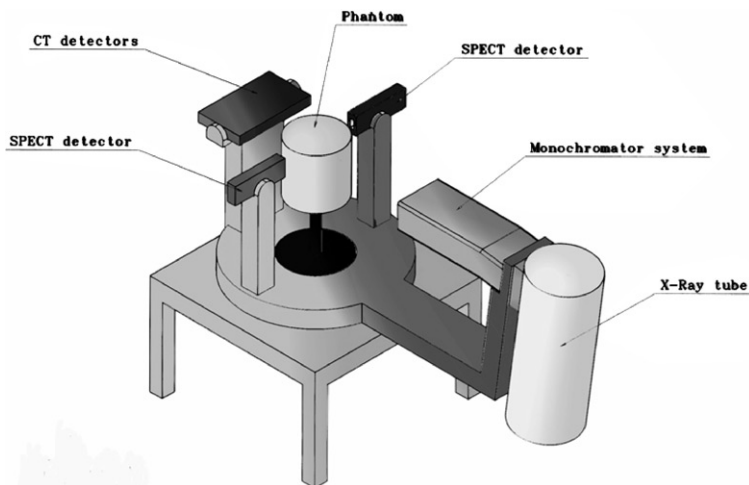


Fig. 1. Schematic of the integrated CT–SPECT system.



Fig. 2. Radiograph of the quasi-monochromatic beam used for CT scans.

integration via tunable capacitors and analog-to-digital conversion. Based on the dynamic range required by our application, a capacitor value of 22 pF was chosen. All the boards use the same clock signal at 10 MHz and are interconnected to allow multiple DDC112 units to be cascaded. The 20-bit digital signals were fed into a PC via parallel port. A software in C language was specifically written to control the integration time and to provide the trigger for starting data acquisition and retrieval.

A lead collimator having an aperture of 3 mm is placed at the entrance window of the detector, thus giving an actual pixel size of  $1 \times 3 \text{ mm}^2$ .

## 2.2. SPECT detector

The scintigraphic detector (two identical heads) is based on a CsI:Tl matrix coupled to a position sensitive photomultiplier. The scintillator matrix is made up of  $8 \times 8$  match-like crystals,  $2.5 \times 2.5 \times 5 \text{ mm}^3$  of size. The crystal elements are optically isolated from each other by a 0.25 mm reflective layer. The photomultiplier (Hamamatsu, Japan, mod. R5900-C8) has an active area of  $22 \times 22 \text{ mm}^2$ . A high-resolution lead collimator having the following characteristics is placed at the entrance window of the scintillator: hole diameter 1.0 mm, septa thickness 0.2 mm, height 22 mm. The calculated geometrical efficiency is  $2.4 \times 10^{-4}$ . The dimensions of the FOV in SPECT are 2 cm axially and 2 cm in diameter. The energy resolution, measured with a  $^{99m}\text{Tc}$  source and without collimator, is 23% (FWHM) at 140 keV. The same radioactive source was used to measure the integral uniformity, yielding a value of about 3%. Finally, a sensitivity of about 7 cps/ $\mu\text{Ci}$  was experimentally found for each detector head. Details of such measurements can be found in Ref. [6].

## 3. Results and discussion

### 3.1. CT acquisition

CT profiles were recorded by rotating the system with an angular step of  $2^\circ$  from  $0^\circ$  to  $180^\circ$ . The

X-ray tube conditions were 40 kV, 10 mA, and the exposure time was 500 ms for all acquisitions. The following data processing must be applied to the raw profiles to obtain the corrected sinogram:

- (1) dark and white field normalization,
- (2) calculation of  $-\ln(I/I_0)$ ,
- (3) centering of sinogram.

The first correction which was applied to each profile was for dark and white field. The dark field is the signal which is measured in the absence of X-rays and includes both true dark current and ADC pedestal offset contribution. The white field is the profile which is measured with the X-rays on, but without any object between the X-ray tube and the detector. The pattern in the white field profile includes the contribution of non-uniformities in the incident quasi-monochromatic X-ray beam (see Fig. 2) and uneven response of UFC detectors. Both dark and white field profiles were obtained by averaging 100 acquisitions. The two mean profiles used for profile correction are plotted in Fig. 3. The corrected profile  $p_{\text{corr}}$  is given by

$$p_{\text{corr}} = (p_{\text{raw}} - p_{\text{dark}})/(p_{\text{white}} - p_{\text{dark}}) \quad (1)$$

where  $p_{\text{raw}}$  is the acquired profile,  $p_{\text{dark}}$  is the average dark profile and  $p_{\text{white}}$  is the average white profile. The corrected sinogram is obtained by taking the negative logarithm of the ratio of the transmitted intensity  $I$  to the intensity in the air  $I_0$  outside the object for each profile. The raw and the corrected sinograms are shown in Fig. 4.

For the reconstruction of tomographic data, it is necessary to precisely determine the position of the rotation axis with respect to the digital data array. To this aim we measured the so-called center of rotation (COR) which was obtained by acquiring a  $270^\circ$  rotational sinogram of a high attenuating point-like object positioned near the physical axis of rotation. The measured offset between the center of the data array and the center of the rotation axis was then used in the reconstruction program.

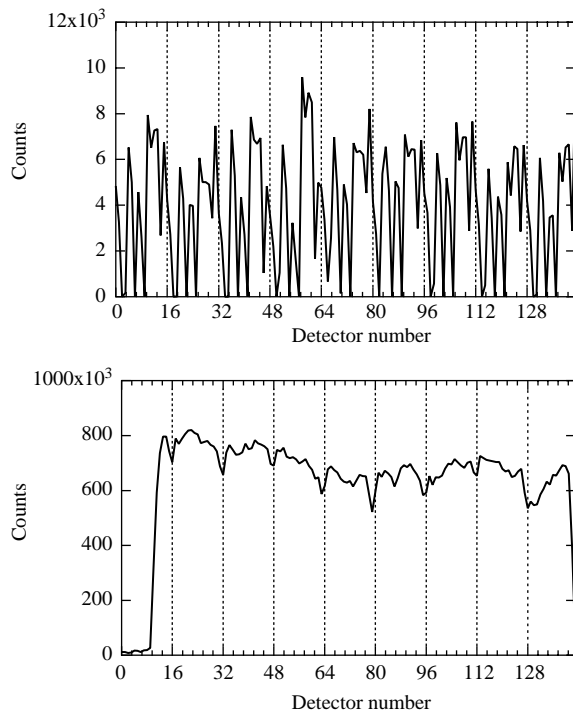


Fig. 3. Average dark profile (top) and white profile (bottom).

### 3.2. SPECT acquisition

SPECT images were acquired by rotating the system with an angular step of 6 degrees from  $0^\circ$  to  $180^\circ$ . The acquisition time of each view was about 1 min and the data were stored in list mode. The data correction was performed by using three look-up tables that account for:

- (1) the spatial non-linearity of PSPMT, i.e., the spatial distortions due to PSPMT were corrected via the appropriate algorithm (see Fig. 5);
- (2) the uneven response of both CsI crystal and PSPMT, i.e., the 140 keV peak-shift of each detector element was corrected by applying a normalization procedure;
- (3) the variation of detection efficiency within the scintillator matrix, i.e., the number of events detected by each element was corrected by using the image of a uniform (flood) radioactive source.

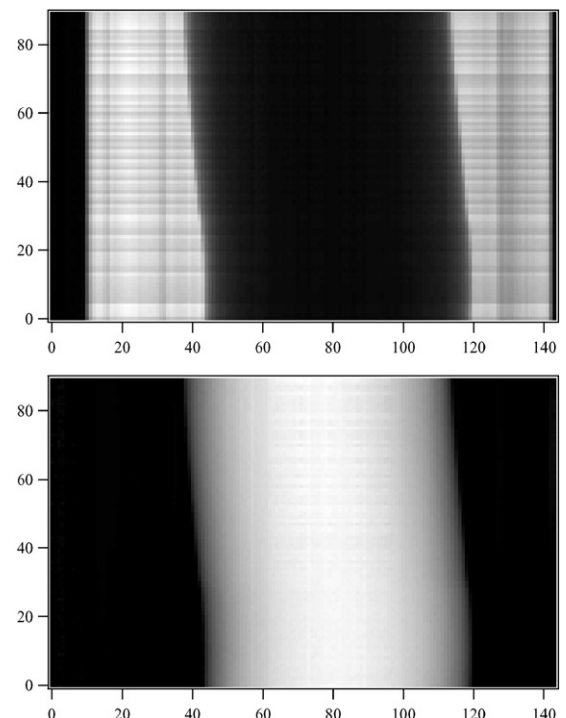


Fig. 4. CT acquisition of a cylindrical phantom: raw sinogram (top), corrected sinogram (bottom). (For the correction procedure: see text.)

As for CT acquisition, a similar procedure for determining the COR of the SPECT system was carried out before acquiring the data.

### 3.3. Image reconstruction and fusion

The CT sinograms were reconstructed by means of the RECLBL library [9] using the conjugate gradient method of reconstruction. We chose this reconstruction program because it takes into account the fan-beam geometry using a flat detector. With the Unix platform we used, the maximum reconstruction time was always less than 1 min.

As far as the SPECT image reconstruction is concerned, an iterative method (simulated annealing) was applied. The algorithm made use of the attenuation coefficients obtained from the CT image and of the corresponding coefficients at the energy of 140 keV that we calculated by means of an analytical function.

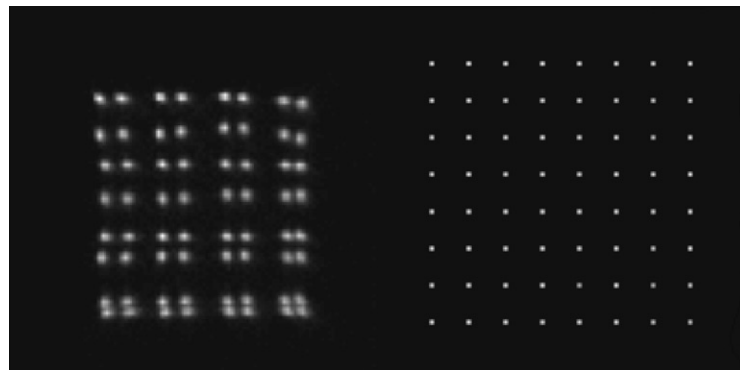


Fig. 5. Correction of spatial distortion in SPECT: raw matrix (left), matrix corrected using the appropriate look-up table (right).

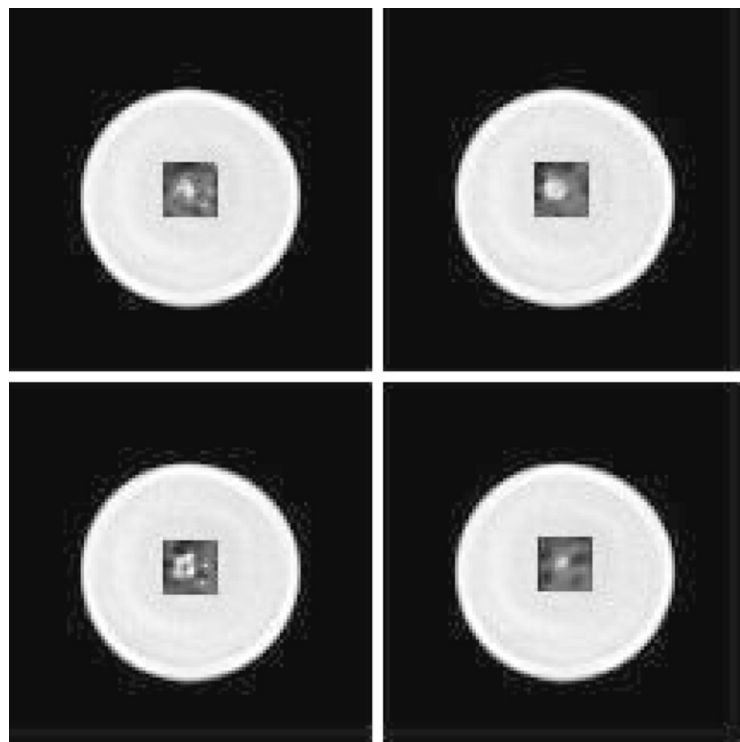


Fig. 6. Fusion of CT and SPECT images.

Finally, the fusion of CT and SPECT images was performed by equal weighing the two contributions. The fused image of a test phantom is shown in Fig. 6. A complete description of the phantom has been previously reported [6]. Briefly, it consists of two coaxial plexiglas cylinders with the outer cylinder filled with a hydro-alcoholic solution labelled with  $^{99m}\text{Tc}$  to

simulate the breast tissue and the inner one filled with water labelled with a higher concentration of  $^{99m}\text{Tc}$  to simulate a tumour. It is worth noting that the developed CT-SPECT prototype is able to detect a region of interest of  $1\text{ cm}^3$ , with a 10:1 tumour/background concentration ratio, within an object having a diameter of 8 cm.

Preliminary results have demonstrated the feasibility of the combined CT–SPECT tomograph. However, before testing the system prototype in a clinical environment, various issues have to be addressed. The SPECT FOV must be enlarged so as to reconstruct full size images as in CT modality. Furthermore, the use of more sophisticated fusion algorithms is desirable for better lesion detection and display. Finally, the diagnostic limits of such a technique have to be investigated by means of more complex tomographic phantoms.

#### 4. Conclusions

A prototype of combined CT–SPECT tomograph has been assembled and evaluated. Images of a test phantom have been reconstructed with both modalities. The CT–SPECT images fusion has been successfully implemented. Work is in progress to enlarge the SPECT FOV.

#### Acknowledgements

Work developed within the 2-year project “Combined Emission–Transmission Tomography for Breast Cancer Study”, MURST—COFIN 1998.

#### References

- [1] E.D. Pisano, C.A. Parham, Radiol. Clin. North Am. 38 (2000) 861.
- [2] M. Säbel, H. Aichinger, Phys. Med. Biol. 41 (1996) 315.
- [3] I. Khalkhali, et al., J. Am. Colloid. Surg. 178 (1994) 491.
- [4] F. Scopinaro, et al., Eur. J. Nucl. Med. 21 (1994) 984.
- [5] F. Scopinaro, et al., Eur. J. Nucl. Med. 26 (1999) 1279.
- [6] M. Gambaccini, et al., IEEE Trans. Nucl. Sci. 48 (2001) 703.
- [7] M. Gambaccini, et al., Phy. Med. XVII, (2001) 249.
- [8] R. Hupke, C. Doubrava, Phys. Med. XV (1999) 315.
- [9] R.H. Huesman, G.T. Gullberg, W.L. Greenberg, T.F. Budinger, RECLBL Library Users Manual, Lawrence Berkeley Laboratory, University of California, 1997.